

# Tm:Ti:LiNbO<sub>3</sub> Waveguide for Quantum Memory Applications

M. George, R. Ricken and W. Sohler  
 Angewandte Physik, Department Physik  
 Universität Paderborn, Paderborn, Germany  
 mathew.george@uni-paderborn.de

E. Saglamyurek, N. Sinclair, C. La Mela and W. Tittel  
 Institute for Quantum Information Science,  
 and Department of Physics and Astronomy  
 University of Calgary, Calgary, Canada

**Abstract**—We report fabrication and characterization of a Tm:Ti:LiNbO<sub>3</sub> optical waveguide, single mode around 800 nm wavelength, in view of photon-echo quantum memory applications. In particular, room- and low-temperature properties were investigated via loss and absorption measurements, spectral hole burning, photon echo, and Stark spectroscopy.

**Keywords:** rare-earth-ion doped crystal; optical waveguide; lithium niobate; photon-echo; quantum memory.

## I. INTRODUCTION

Quantum memories are key elements for quantum repeaters, which promise overcoming the distance barrier of quantum communication [1]. A currently extensively studied approach relies on photon echoes [2,3]. Tm:Ti:LiNbO<sub>3</sub> optical waveguides combine interesting features arising from the specific rare-earth dopant, the host material, as well as the waveguide. Specifically, thulium features a transition at 795 nm (Fig. 1), a wavelength where air is transparent, entangled photons are conveniently generated in non-linear crystals or optical fibres, and high-efficiency and easy-to-operate single photon detectors are commercially available. Furthermore, when implemented into Lithium Niobate, its electronic states acquire permanent electric dipole moments, allowing for modification of the transition frequencies through the application of an electric field [4]. Finally, the use of a waveguide where travelling wave electrodes can be spaced closely and light intensities can be large, promise simple integration with fibre optics and quantum networks, sub-ns Stark frequency control, and large Rabi frequencies, which benefits the optical pumping procedure required for spectral tailoring of the inhomogeneously broadened absorption line [2,3].

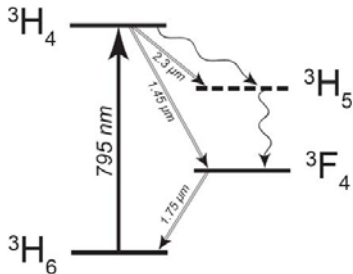


Figure 1. Simplified energy level diagram of Tm:LiNbO<sub>3</sub> showing the electronic levels relevant to this work.

## II. WAVEGUIDE FABRICATION AND CHARACTERIZATION

### A. Tm diffusion doping of LiNbO<sub>3</sub>

Commercially available 0.5 mm thick Z-cut wafers of undoped optical grade congruent lithium niobate were Tm-doped near the +Z-surface before waveguide fabrication. A vacuum deposited Tm layer of 19.6 nm thickness was in-diffused at 1130 °C during 150 hrs in an argon-atmosphere followed by a post treatment in oxygen (1 h). The diffusion profile was determined by secondary neutral mass spectroscopy (Fig. 2). The maximum Tm concentration of about  $1.35 \times 10^{20} \text{ cm}^{-3}$  corresponds to a concentration 0.74 mole %.

### B. Ti indiffused waveguides in Tm:LiNbO<sub>3</sub>

On the Tm-doped surface 3.0 μm wide, 40 nm thick Ti-strips were deposited and subsequently in-diffused at 1060 °C for 5 hrs to form 30 mm long optical strip waveguides. In the wavelength range around 775 nm, these waveguides are single mode for TE and TM-polarization (see also Fig. 2).

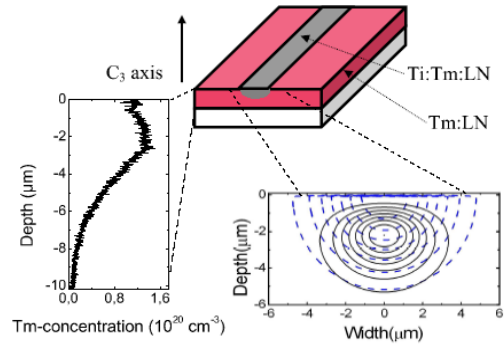


Figure 2. Scheme of the waveguide geometry with the measured Tm concentration profile on the left and the calculated intensity distribution of the fundamental TM-mode superimposed on the profile of the extraordinary index of refraction induced by the Ti-doping. The latter data are for 795 nm wavelength. Iso-intensity lines are plotted for both, the index and the mode profile, corresponding to 100%, 87.5%, 75% etc. of the maximum index increase ( $\Delta n_{max} = 4.0 \times 10^{-3}$ ) and mode intensity, respectively.

### C. Characterization

The total waveguide propagation losses, consisting of absorption and scattering loss, were measured around 800 nm wavelength at room temperature by the Fabry-Perot method [5]. In addition, the waveguide propagation loss was determined at 729 nm wavelength where negligible absorption by the Tm-

ions is expected. In this way the scattering loss was determined alone; it is 0.2 dB/cm for both polarizations.

Moreover, polarization dependent transmission spectra of a 30 mm long waveguide were measured, yielding the inhomogeneously broadened spectrum depicted in Fig. 3.

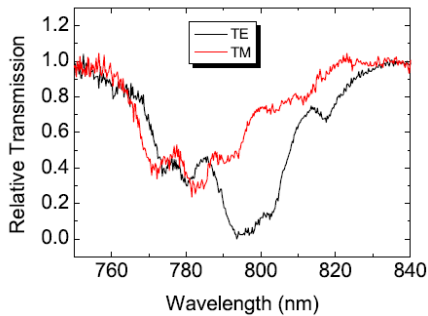


Figure 3. Relative transmission through the Tm:Ti:LiNbO<sub>3</sub> waveguide for TM- and TE-polarization, respectively, as a function of wavelength.

### III. THULIUM SPECTROSCOPY

To characterize Tm:Ti:LiNbO<sub>3</sub> waveguides for photon-echo based quantum memories, we studied a large variety of low-temperature (3K) properties (for more information see [6,7]).

First, we repeated the measurement of the inhomogeneously broadened  $^3H_6 \leftrightarrow ^3H_4$  absorption line at 3.5 K, which confirmed the strong polarization dependence that we already found at room temperature. Furthermore, the measurement reflected the temperature dependent distribution of atomic population in the ground state Stark levels, and enhanced absorption for transitions starting in the ground state Stark level.

Next, we investigated relaxation avenues and population dynamics of the  $^3H_4$  and  $^3F_4$  atomic. This impacts on the possibility to tailor the inhomogeneously broadened absorption line by frequency selectively transferring absorbers to long-lived states. Figure 4 depicts the results of time-resolved spectral hole burning, yielding radiative lifetimes of 82  $\mu$ s and 2.4 ms for the  $^3H_4$  and  $^3F_4$  levels, respectively, and a branching ratio from the  $^3H_4$  into the  $^3F_4$  level of  $\sim 44\%$ .

We repeated these studies under application of magnetic fields between 100 and 1250 Gauss, oriented parallel to the crystal C<sub>3</sub>-axis. This led to the appearance of two atomic ground state sub-levels with lifetimes exceeding 1 second.

An important property that determines the storage time of quantum states in optical atomic is the width of the sharpest spectral feature that can be generated. It depends on the homogeneous linewidth of the  $^3H_6 \leftrightarrow ^3H_4$  transition (which itself is limited by the inverse radiative lifetime) as well as on spectral diffusion, which leads to time dependent broadening. Using two- and three-pulse photon echoes, we found an effective homogeneous linewidth of 1.082 MHz, and hence a minimum spectral feature of around 2 MHz.

Finally, in order to control dephasing and rephrasing of atomic coherence through electric fields [2], we measured the DC Stark effect, again using spectral hole burning techniques. We

observed a linear frequency shift (reflecting the symmetry properties of Tm in LiNbO<sub>3</sub>) of  $24.6 \pm 0.7$  kHz/cm/V.

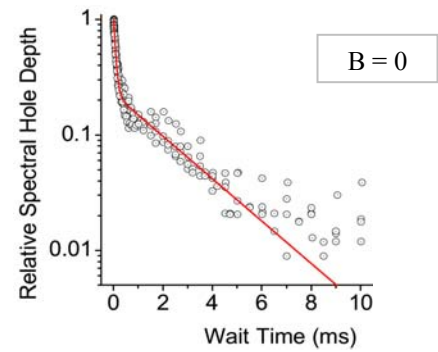


Figure 4. Spectral hole decay under zero magnetic field. Plotted circles denote the normalized spectral hole depth as a function of the waiting time between burning and reading pulses. Two exponential decays are easily identified, yielding radiative lifetimes of 82  $\mu$ s and 2.4 ms for the  $^3H_4$  and  $^3F_4$  levels, respectively. The branching ratio into the  $^3F_4$  level is approximately 44%.

### IV. CONCLUSIONS

Our findings demonstrate the suitability of Tm:Ti:LiNbO<sub>3</sub> waveguides cooled to 3 K for implementations of photon-echo quantum memory protocols. Level structure, lifetimes, and branching ratios allow tailoring of the natural, inhomogeneously broadened absorption profile. The minimum width of spectral holes of  $\sim 2$  MHz, as determined by spectral diffusion, will limit storage of quantum information in optical coherence to roughly a hundred nanoseconds. While longer times may be achievable at lower temperature, this is still sufficient for mapping coherence onto long-lived ground state coherence, as Rabi frequencies exceeding hundred MHz can be obtained, due to the high power densities achievable inside waveguiding structures. Finally, the existence of a linear Stark shift, together with the possibility to space electrodes closely, allows shifting of resonance frequencies by more than 100 MHz within sub-nanosecond times, thus enabling novel phase control techniques. The first demonstration of a quantum memory protocol, using this waveguide, will be reported elsewhere [8].

### REFERENCES

- [1] H. J. Briegel, W. Dür, J. I. Cirac and P. Zoller, “Quantum repeaters: The role of imperfect local operations in quantum communications,” *Phys. Rev. Lett.* 81, 5932 (1998).
- [2] W. Tittel *et al.*, “Photon-echo quantum memory in solid state systems” *Laser and Photonics Rev.* DOI 10.1002/lpor.200810056.
- [3] H. de Riedmatten *et al.*, “A solid-state light-matter interface at the single-photon level,” *Nature* 456, 773 (2008).
- [4] R. Macfarlane, “Optical Stark spectroscopy of solids,” *J. Lumin.* 125, 156 (2007).
- [5] R. Regener and W. Sohler, “Loss in low-finesse Ti:LiNbO<sub>3</sub> waveguide resonators” *App. Phys. B*, vol 36 p 143 (1985).
- [6] N. Sinclair *et al.*, “Spectroscopic investigations of a Ti:Tm:LiNbO<sub>3</sub> waveguide for photon echo quantum memory”, *J. Lumin.*, in press.
- [7] C.W. Thiel *et al.*, “Optical Decoherence and Persistent Spectral Hole Burning in Tm<sup>3+</sup>:LiNbO<sub>3</sub>”, *J. Lumin.*, in press.
- [8] E. Saglamyurek *et al.*, “Integrated quantum memory for quantum communication”, to be presented at OFC 2010.